Reaction Kinetics and Simulations for Solid-State Polymerization of Poly(ethylene terephthalate)

Dacheng Wu,* Feng Chen, and Ruixia Li

Light Industry and Textile College, Sichuan Union University, Chengdu 610065, China

Youdong Shi

Yizheng Chemical Fiber Limited Company, Jiangsu, Yizheng 211451, China

Received August 19, 1996; Revised Manuscript Received July 11, 1997[⊗]

ABSTRACT: A comprehensive model for solid-state polymerization of poly(ethylene terephthalate) was developed from analyzing the similarities and the differences between solid-state and melt polymerization. Considering the end groups diffusion limitation and the modification of concentrations of end groups and byproducts in the amorphous phase, a system of mass transfer and balance equations suitable for the solid-state polymerization of PET were obtained, based on simplifying the reaction kinetics of melt polymerization of PET. The degradation and other side reactions neglected in the earlier models for the solid-state polymerization of PET were included in the model. This simulation gave a quantitative prediction in the effect of temperature, particle size, starting molecular weight, and ratio of end groups on the degree of polymerization of products during the solid-state polymerization of poly(ethylene terephthalate). These simulation results were in agreement with experiments.

Introduction

The solid-state polymerization (SSP) of poly(ethylene terephthalate) (PET) as a powerful way to enhance its average molecular weight has been of great interest to polymer chemists and engineers for many years.[1−11] The state of the art for SSP of PET was reviewed by Pilati[12] several years ago. Bamford and Wayne[1] considered that in solid-state polymerization the main reaction is only the transesterification reaction and the reaction mechanism is similar to the situation in melt polymerization. In order to explain the effect of particle sizes, Ravindranath and Mashelka[2] developed a model based on the diffusion limitation of byproducts. Considering the transesterification and esterification reactions, Zimmerman et al.[3] proposed a kinetics model and obtained some interesting results. It is noted also that Chen and Chen[4] studied the SSP of PET at different temperatures by the diffusion limitation of end groups.

In fact, the reaction temperature in SSP is usually much lower than that in the melt process and the thermal degradation will be greatly reduced. As a result, the final product of SSP has the low level of some side products, such as carboxyl groups, vinyl groups, and acetaldehyde, which are harmful to the product quality.[5,6] For calculating the rate of each reaction occurring in the solid state, the rate constants obtained from melt polycondensation data can be used. On the other hand, it should consider the difference between melt and solid states. First of all, the mobility of the macromolecular chain in the solid state is much lower than in the melt state, which retards reactions between two macromolecules;[9] therefore, it is necessary to involve the effect of the diffusion limitation of end groups on the reaction rates. In order to avoid the sticking of the prepolymer powders, the crystallinity of the sample should be as high as 40%.[6] The high crystallinity will lead to an increase in the concentration of end groups and byproducts in the amorphous region,[10] because all of end groups or byproducts are located in the amorphous phase principally. Hence, concentrations of end groups and byproducts must be modified in the consideration of the SSP kinetics. According to the above discussion, a comprehensive model for SSP of PET is necessary to involve the diffusion limitation of end groups and byproducts as well as the modification of concentration in the amorphous phase. In addition to the transesterification and esterification reactions, degradation and other side reactions were included in the model.

In this work, the SSP of PET was investigated both experimentally and theoretically. The reaction mechanism for SSP of PET was suggested from analyzing the similarities and the differences between solid-state and melt polymerization. A system of mass transfer and balance equations suitable for SSP of PET were obtained, based on the reaction kinetics of PET polymerization. The simulation results were in agreement with experiments, and some experimental phenomena observed here were explained by the model. Moreover, the character and side product moieties of final products were also investigated.

Theoretical Section

Reaction Mechanism. The SSP of PET is usually carried out at a temperature below its melting point, 10−50 °C lower. However, in principle, all reactions involved in the melt polymerization are possible also in SSP. The rate of every reaction, of course, is obviously different for the two states due to the difference in the reaction temperature, kind and concentrations of end groups, and states of reactants. Therefore, these reactions should be reexamined and simplified properly. According to the early study of Ravindranath et al.,[13] most reactions in the melt polymerization of PET are summarized as follows:

Hovenkamp[14] and Hornof[15] studied the formation kinetics of diethylene glycol (DEG), afforded by reactions 6 and 7 in the melt state and concluded that DEG is formed mainly during the final stage of transesterification and the initial stage of polycondensation. In

* To whom correspondence should be addressed.

[⊗] Abstract published in *Advance ACS Abstracts,* September 15, 1997.

S0024-9297(96)01254-5 CCC: $14.00

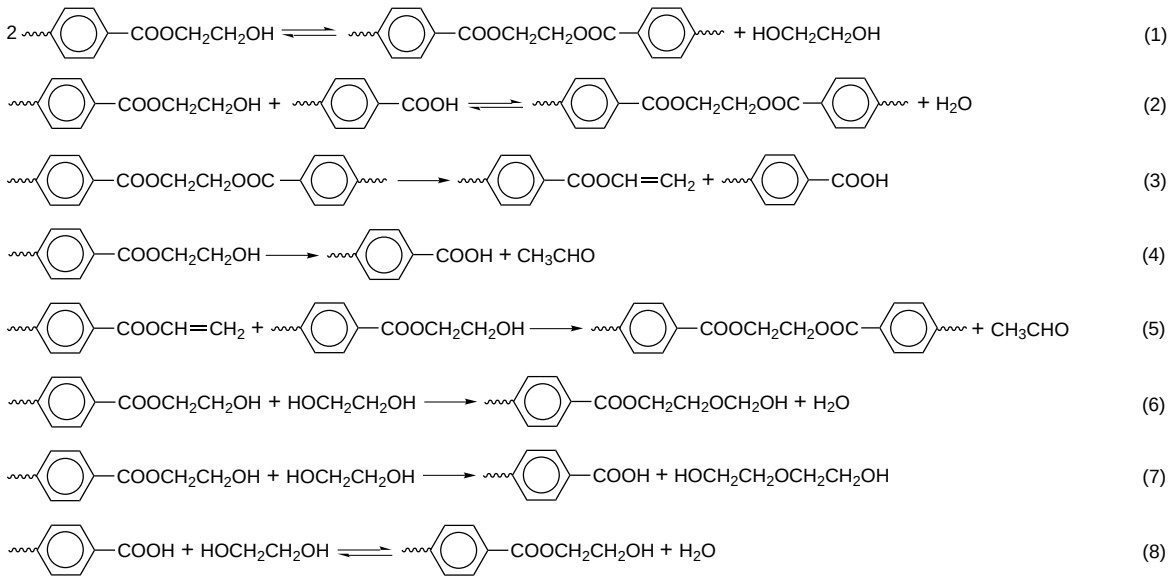

another paper, Wu et al.[16] investigated the change in the concentration of DEG and founded that the moiety of DEG hardly changes during SSP of PET. As a result, we considered that reactions 6 and 7 could be neglected in the case of SSP of PET. Concerning reactions 8 and 2, because the concentration of glycol is 10^2-10^4 times lower than that of the hydroxyl end group, it is correct to ignore the influence of reaction 8 on SSP process. One of the most vital problems in melt-state polymerization of PET is the formation of chromophoric substances that lead to colored final products.[17] The chromophoric substances are mainly poly(enealdehyde)s from acetaldehyde and polyene.[18] However, in the solid state, the concentration of acetaldehyde is only a few ppm, contrary to several tens in the melt state.[5] In conclusion, it is reasonable that only reactions 1−5 should be included in the mechanism of SSP. These reactions (1)−(5) are rewritten by simple symbols, as follows:

$$2Y \rightleftharpoons E + G \qquad (1')$$

$$Y + Z \rightleftharpoons E + W \qquad (2')$$

$$E \rightarrow Z + V \qquad (3')$$

$$Y \rightarrow Z + D \qquad (4')$$

$$V + Y \rightarrow E + D \qquad (5')$$

In the following theoretical deduction, symbols y, z, v, g, w, e, and d indicate concentrations of Y, Z, V, G, W, E, and D, respectively, k_i are rate constants of the ith reaction in the melt polymerization and R_{iS} are rate expressions of the ith reaction in SSP, K_1, and K_2 are equilibrium constants of reactions 1 and 2.

Reaction Rates in SSP. Since the diffusivity of segments of a polymer chain in the solid state is much lower than that in the melt state, the rate of the reaction between two macromolecules should be affected by the diffusion limitation of end groups when the reaction is carried out in the solid state. In order to describe the effect of the end group diffusion limitation on the reaction and to deduce the expression of reaction rate in SSP of PET, we selected a method similar to the analysis of a free radical polymerization by Chiu et al.[19] Clearly, in Figure 1, illustrating a small sphere with the radius r_m, one end of a polymer chain is located at the center of this sphere. The collision and then the possible reaction between two end groups located in this specific volume of the sphere could occur by means of not the transportation of the whole chain but the diffusion of chain ends. In the region of the sphere, the concentration of end groups decreases during reactions of end groups; on the other hand, at a large distance r_D far from the central end group, it approaches the bulk concentration y_b, which is larger than the average concentration within the sphere. Because the difference in concentrations causes end groups to diffuse into this sphere, after reaching a steady state, the concentration c_m of end groups in the sphere becomes constant, and its value could be obtained by canceling out the diffusion and the reaction.

If D is the diffusion coefficient of end groups of a polymer molecule, it is easy to deduce the diffusion rate K of hydroxyl end groups into the sphere with the radius r_m as

$$K = 4\pi D r_m (y_b - y_m) \qquad (9)$$

The net rate of reaction of hydroxyl end groups during the reversible transesterification in the sphere is the same as its rate of diffusion at a steady state, hence,

$$^4/_3\,\pi r_m^3 k_1 (y_m^2 - 4ge/K_1) = K \qquad (10)$$

Equations 9 and 10 yield y_m as

$$y_m = -\frac{1}{2k_1\theta} + \sqrt{\frac{1}{4k_1^2\theta^2} + \frac{y_b}{k_1\theta} + \frac{4ge_0}{k_1}} \qquad (11)$$

where the parameter θ is defined as

$$\theta = \frac{r_m^2}{3D} \qquad (12)$$

which has the dimension of time. Physically, it is equal to one-third of the time during which an end group diffuses at the mean square-root distance equal to $(r_m^2)^{1/2}$.

In the whole system, the rate of reaction 1 in SSP can be written as formally

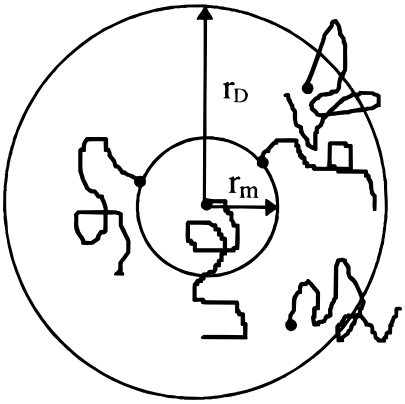

Figure 1. Schematic diagram illustrating the coordinate system used in describing solid-state polymerization.

$$R_{1S} = k_1(y_m^2 - 4ge/K_1) \tag{13}$$

Substituting eq 12 into eq 13 leads to

$$R_{1s} = \frac{y_b}{\theta} - \frac{1}{2k_1\theta^2} + \frac{1}{\theta}\sqrt{\frac{1}{4k_1^2\theta^2} + \frac{y_b}{k_1\theta} + \frac{4ge_0}{k_1}} \tag{14}$$

In semicrystalline PET, it was assumed that end groups and volatile small molecules are concentrated in the amorphous region. If ϕ_C is the crystallinity of PET particles, it is easy to make a modification of the concentration by writing

$$\text{effective concentration} = \text{average concentration}/(1 - \phi_C) \tag{15}$$

Modifying the rate expression eq 14, by the effective concentration of eq 15, we obtain

$$R_{1s} = \frac{y_b}{\theta} - \frac{(1-\phi_c)}{2k_1\theta^2} + \frac{(1-\phi_c)}{\theta}\sqrt{\frac{1}{4k_1^2\theta^2} + \frac{y_b}{k_1\theta(1-\phi_c)} + \frac{4ge}{K_1(1-\phi_C)}} \tag{16}$$

For reactions 2 and 5, like reaction 1, we can write R_{2S} and R_{5S} as

$$R_{2S} = \frac{k_2}{1 + \theta k_2 z_b}\left(\frac{yz}{1-\phi_c} - 2\,we/K_2\right) \tag{17}$$

$$R_{5S} = \frac{k_5}{1 + \theta k_5 v_b}\left(\frac{yv}{1-\phi_c}\right) \tag{18}$$

There is not the end group diffusion limitation for reactions 3 and 4, hence,

$$R_{3S} = k_3 e \tag{19}$$

$$R_{4S} = k_4 y \tag{20}$$

Mass Transfer and Balance Equations. The shape of PET particles in the sample is assumed to be spherical for the convenience of modeling. Individual mass transfer and balance equations of the reaction system are obtained as follows:

$$\frac{\partial y}{\partial t} = -(2R_{1S} + R_{2S} + R_{4S} + R_{5S}) \tag{21}$$

$$\frac{\partial z}{\partial t} = -R_{2S} + R_{3S} + R_{4S} \tag{22}$$

$$\frac{\partial v}{\partial t} = R_{3S} - R_{5S} \tag{23}$$

$$\frac{\partial g}{\partial t} = D_g\left(\frac{\partial^2 g}{\partial r^2} + \frac{2}{r}\frac{\partial g}{\partial r}\right) + R_{1S} \tag{24}$$

$$\frac{\partial w}{\partial t} = D_w\left(\frac{\partial^2 w}{\partial r^2} + \frac{2}{r}\frac{\partial w}{\partial r}\right) + R_{2S} \tag{25}$$

$$\frac{\partial d}{\partial t} = D_d\left(\frac{\partial^2 d}{\partial r^2} + \frac{2}{r}\frac{\partial d}{\partial r}\right) + R_{4S} + R_{5S} \tag{26}$$

where R_{iS} are obtained from equations 16−20. The boundary conditions are

$$g = w = 0, \quad \text{for} \quad r = R \tag{27}$$

$$\frac{\partial g}{\partial r} = \frac{\partial w}{\partial r} = 0, \quad \text{for} \quad r = 0 \tag{28}$$

The initial conditions for the mass transfer and balance equations are

$$z_0 = 2.96 \times 10^{-5}\ \text{mol/cm}^3 \tag{29}$$

$$e_0 = 7.26 \times 10^{-3}\ \text{mol/cm}^3 \tag{30}$$

The value of y_0 is calculated from the number-average molecular weight and initial values of concentrations of end groups. In addition, the initial concentrations g_0, w_0, and v_0 are set at zero.

Numerical Calculation. The mass transfer and balance equations are a set of partial differential equations to which Crank−Nicholson's[20] finite difference method could be applied for the numerical solution. From equation 14, the rate of reaction 1 in the solid state depends on $r_m^2/3D$, and it can be written in analogy with the discussion of Chiu et al.[19] as

$$\frac{r_m^2}{3D} = \frac{r_m^2}{3D_0}\frac{D_0}{D} = \Theta\frac{D_0}{D} \tag{31}$$

where D_0 is the diffusivity at the reference state. It can be obtained from WLF equation

$$\log\frac{D_0}{D} = \frac{-17.4_1(T - T_g)}{51.6 + T - T_g} \tag{32}$$

where T_g is the glass transition temperature of PET, i.e., 78 °C.

In order to solve the set of mass transfer and balance equations, the parameter values used in the calculation were obtained from the literature.[10,13,21,22] It should be emphasized that the value of the parameter Θ may be introduced only as an empirically fitting factor in the calculation because of the difficulty in estimating this value theoretically.

Since the molecular weight M_n is a function of temperature T and position r, its distribution function $M_n(r)$ can be expressed at a certain temperature as

$$M_n(r) = 2 \times 192e_0/[y(r) + z(r) + v(r)] \tag{33}$$

Table 1. Intrinsic Viscosity ([η], dL/g) of PET as a Function of Reaction Time at Different Temperatures and Particle Sizes

temp (°C)	particle sizes (mm)	heating time (min)				
		0	8	15	30	60
245	0.25	0.671	0.685	0.706	0.764	0.870
235	0.5	0.588	0.600	0.605	0.613	0.627

The average value of M_n, i.e., the number-average molecular weight M_n, is calculated from the following equation according to its definition.

$$\frac{1}{\bar{M}_n} = \frac{\int_0^R [4\pi r^2/M_n(r)]\, dr}{4\pi R^3/3} \tag{34}$$

Experimental Section

Materials. The PET prepolymers were supplied by Yizheng Chemical Fiber Limited Co. They were prepared from ethylene glycol and dimethyl terephthalate using Sb_2O_3 as catalyst by the melt-condensation process. Before the SSP process, the chips of PET were broken into 10−20 mesh particles by a broken machine, the particles were powdered further by low-temperature air jet and then sieved.

Procedure of the Solid State Polymerization. The reaction apparatus for the SSP involved a series of six reaction tubes, which were connected to a vacuum line to reach a vacuum of 50−150 Pa and immersed in a salt bath having constant temperature with a precision ±2 °C. The SSP process of PET included three stage, i.e., drying, polycondenation, and cooling. The drying process was carried out a temperature 170 °C for 90 min, and the polycondensation process at temperatures 215, 225, 235, and 245 °C, respectively.

The drying process not only decreased the concentration of water in PET resin but also, more importantly, increased the crystallinity of prepolymers, which was beneficial to prevent particles from sticking.[6] Remelting of PET chips usually leads to the decrease in molecular weight because of the hydrolysis of polymer chains. So, the careful removal of water in the prepolymer particles is very important in order to avoid the degradation caused by water. In our experiment, drying for 90 min at 170 °C was sufficient to remove water and eliminated any question of hydrolysis. This conclusion was proved by the determination of the molecular weight of samples at early stage of SSP indicated in Table 1.

Average Molecular Weight of PET. The intrinsic viscosity [η] was measured by an Ubbelohde viscometer with the mixture of tetrachloroethane and phenol (1 to 1, w/w) as the solvent at 25 ± 0.02 °C. The value of [η] was obtained by the five-point method, and M_n was calculated from the intrinsic viscosity by the empirical relation $[\eta] = 2.1 \times 10^{-4} M_n^{0.82}$.

Determination of Carboxyl End Groups. Carboxyl end groups were determined by acidimetric titration in a phenol−chloroform (1:1, v/v) mixture at 80−100 °C. The alkaline solution used was 0.1 M potassium hydroxide in benzyl alcohol, and the indicator was bromphenol blue.

Crystallinity Measurements. The apparent degree of crystallinity ϕ_c expressed as a volume fraction, was calculated from density measurements using the relation

$$\phi_c = \frac{\rho - \rho_a}{\rho_c - \rho_a} \tag{35}$$

where ρ presents the density of samples, ρ_c is the density of the prefect crystal, $\rho_c = 1.455$ *g*/cm^3 at 25 °C, and ρ_a is the density of amorphous PET, $\rho_a = 1.355$ *g*/cm^3 at 25 °C.

Results and Discussion

Determination of Parameter Θ. According to eqs 12 and 30, the parameter Θ is of the clear physical meaning, but it is not easy to obtain its value theoretically. Therefore, it was suggested as a fitting parameter Θ. In order to investigate the dependence of reaction rates on the value of parameter Θ for samples, we selected the temperature 245 °C and particle size 0.25 mm. As shown in Figure 2, the change in M_n during the SSP process depends on the value of parameter Θ. When Θ = 100 min, the simulation results fit best with experimental results. Hence, this value of parameter Θ was selected in the further simulation.

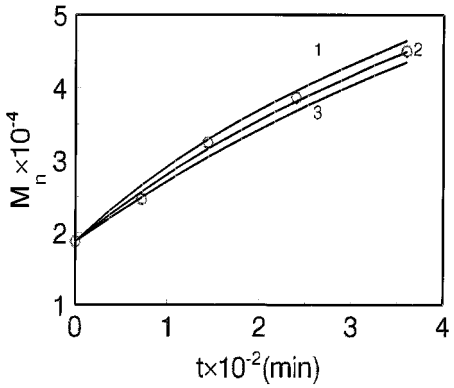

Figure 2. Determination of parameter Θ according to fitting the curve of number-average molecular weight M_n vs time *t* at $T = 245$ °C, $R = 0.25$ mm. Θ (in min): (1) 10; (2) 100; (3) 200; (○) experimental.

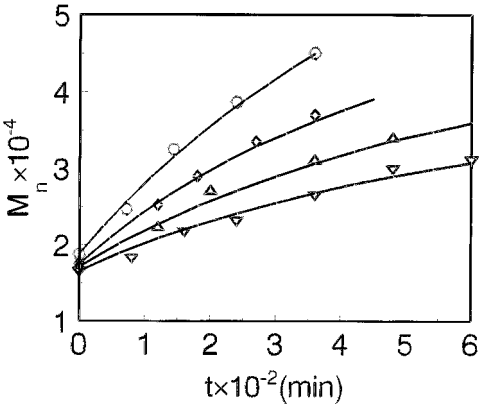

Figure 3. Effect of temperature on the relationship of number-average molecular weight M_n vs time *t*: (○) $T = 245$ °C; (◊) $T = 235$ °C; (△) $T = 225$ °C; (▽) $T = 215$ °C. (—) Simulation, experimental at particle size: $R = 0.25$ mm.

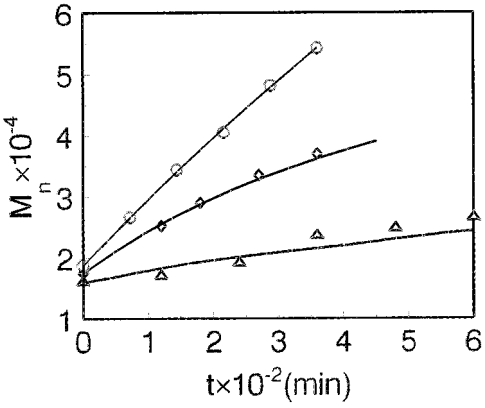

Figure 4. Effect of temperature on the relationship of number-average molecular weight M_n vs time *t*. (—) Simulation, experimental at temperature $T = 235$ °C. Particle sizes: (○) $R = 0.1$ mm; (◊) $R = 0.25$ mm; (△) $R = 0.5$ mm.

Effect of Temperature and Particle size. Figures 3 and 4 show simulating and experimental results for average molecular weights of samples with different particle sizes at different times and temperatures. It

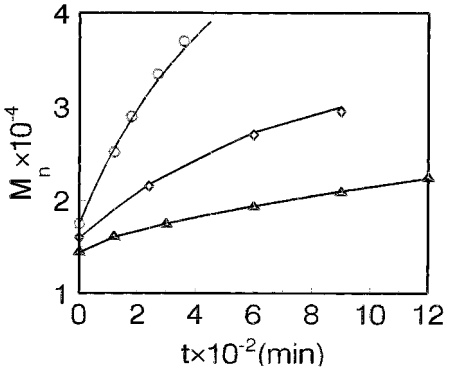

Figure 5. Effect of starting molecular weights on SSP of PET at $T = 235$ °C and $R = 0.25$ mm: (△) $M_n = 14\,400$; (◊) $M_n = 16\,000$; (○) $M_n = 17\,500$.

can be seen that the simulation results are in good agreement with experimental data at different temperatures and particle sizes. The overall rates for SSP of PET increase with increasing temperature and decreasing particle size. These results show that SSP of PET is under the byproduct diffusion limitation, and the decrease in particle size makes the specific surface area of samples large, which is beneficial to the byproduct diffusion. In our treatment, the shape of partcles was suggested as a sphere for the convenience. This concept of equivalent sphere was accepted widely in the literature of chemical engineering. Generally, the diffusion of byproducts is related with the geometrical shape of particles,[2] and the diffusion equations for different shapes have been developed and solved by both theoretical and numerical methods successfully.[7,8,18] It is not difficult to handle the problem of other shapes, e.g., cube and cylinder, with this model. A simple change in the terms of the diffusion equations for byproducts is only necessary. However, further discussion was beyond the scope of this paper.

Starting Molecular Weight and Remelting. Samples of PET particles with different starting molecular weights were subjected to SSP at 235 °C. Reactions of all samples were carried out similarly. Simply speaking, the higher the starting molecular weight, the faster the reaction rates, as shown in Figure 5. It was evident from this that there is an important effect of the starting molecular weight on reaction rates. Buxbaum et al.[17] observed the same phenomenon and explained as the negative influence of crystallinity of PET. In fact, in the solid state, concentrations of glycol and water in the outer shell of a PET particle are lower than those in its center because of the diffusion limitation of byproducts. Therefore, the reaction rates of end groups in the outer shell are faster than that in the center, which leads to the difference in end group concentrations and molecular weight between the outer shell and the center. Figure 6 shows the effect of remelting on the molecular weight−time relationship during SSP. Obviously, in the subsequent 2 or 4 h after starting SSP, the procedure of remelting will increase the molecular weight of PET particles. This simulation was similar to the experimental observation by Gaymans et al.[9]

Concentration Ratio of End Groups. Figure 7 shows the dependence of M_n on the concentration ratio of end groups ([COOH]:[OH]). The value of M_n indicated in that figure was obtained for the sample at $t = 360$ min. Although the concentration ratio of end groups, in the range of this ratio, about 0.5−0.8, greatly increased M_n, this ratio was insensitive to the reaction temperature and the particle size, which was similar

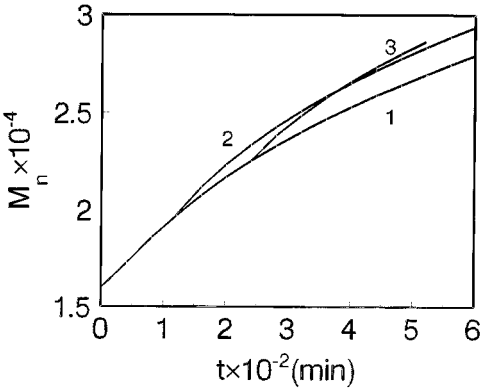

Figure 6. Effect of remelting on SSP of PET at $T = 235$ °C and $R = 0.25$ mm: (1) no remelting; (2) remelting after 120 min; (3) remelting after 240 min.

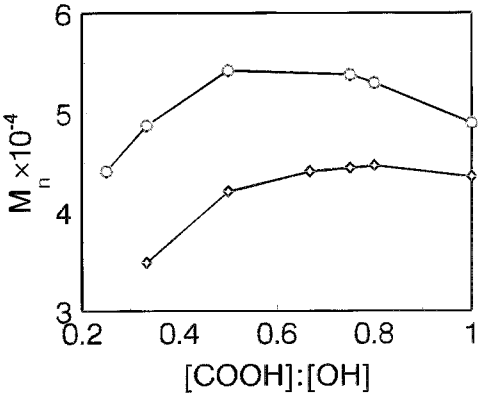

Figure 7. Effect of concentration ratio of end groups on M_n at particle size $R = 0.25$ mm and time $t = 360$ min. Temperatures: (○) $T = 245$ °C; (◊) $T = 225$ °C.

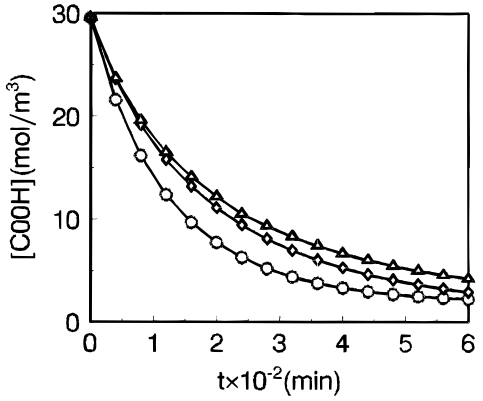

Figure 8. Concentration of carboxyl groups vs time t at different temperatures and particle sizes. Temperatures and particle sizes: (○) $T = 235$ °C, $R = 0.25$ mm; (◊) $T = 225$ °C, $R = 0.25$ mm; (△) $T = 235$ °C, $R = 0.5$ mm.

to the results obtained by Zimermman et al.[3] This indicated that the esterification reaction plays an important role in the process of increasing M_n and is indispensable in the study on SSP of PET.

Change in Carboxyl End Group Concentration. Though the changing rate of M_n increases with the increasing concentration of carboxyl end groups within certain limits, it leads to an increase in these groups, which is harmful for the thermal stability of the final products of PET. Figure 8 shows the variation of the carboxyl end group concentrations with the reaction time at different conditions. It could be seen that the carboxyl end group concentration decreases sharply during the first stage of SSP. This result indicated that

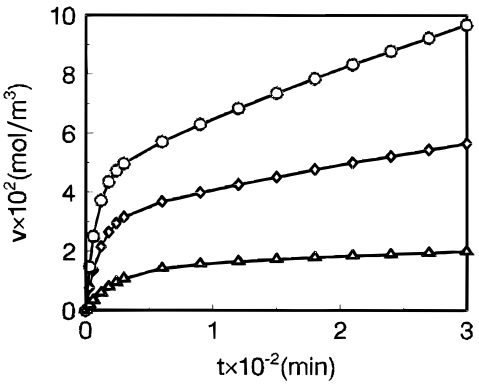

Figure 9. Concentration of vinyl groups vs time t at different temperatures. Particle sizes: $R = 0.25$ mm. Temperatures: (○) $T = 245$ °C; (◇) $T = 235$ °C; (△) $T = 225$ °C.

SSP of PET is an useful method to obtained PET products with the considerable low concentration of carboxyl end groups. Because the variation of [COOH] is parallel to the rate of esterification reaction, the reaction at 235 °C, $R = 0.5$ mm is slower than that at 225 °C, $R = 0.25$ mm, as is shown in Figure 8. On the one hand, the decrease in reaction temperature makes the reaction slow; on the other hand, the decrease in particle size will decrease the byproduct diffusion limitation. The combination of these two factors leads to the above-mentioned results.

Change of Other Side Products. According to reactions 3−5, the important side products in the SSP of PET are carboxyl groups, vinyl end groups, and acetaldehyde. It was so difficult to determine the concentration of vinyl groups in PET resin that we only studied the kinetics of vinyl groups in simulation. As is seen from Figure 9, the concentration of vinyl groups increases with increasing temperature and reaction time. Although the rate of vinyl groups formation is small, they will accumulate after a long time and further lead to formation of anhydride groups, acetaldehyde, or a network.[3] The other kind of side products, acetaldehyde, even at a concentration as low as a few ppm, will cause flavors in soft drinks. However, we cannot obtain a theoretical value of the concentration of acetaldehyde for lack of diffusivity data of acetaldehyde in PET resin. The experimental results obtained by Jabarin et al.[5] show that the moieties of acetaldehyde decrease sharply at the first stage of SSP of PET and depend on particle sizes. It was evident from this that the variations of acetaldehyde residual are controlled by diffusion limitation. They also found that the higher the reaction temperature, the lower the moieties of acetaldehyde. Although the formation rate of acetaldehyde increases with the increase in reaction temperature, the loss rate by diffusion may increase more sharply.

Crystallinity. The crystallinity of PET samples plays an important role in SSP of PET, because it may effect diffusivities of end groups or byproducts. However, there is not now a quantitative relation between these diffusivities and crystallinity. Fortunately, the crystallinity can be assumed constant (the density of final products about 1.385 g/cm^3, the crystallinity ϕ_C about 40%) in solid stating, because the polymerization takes place mostly during the slow second stage where the crystallinity increases slowly. The melting behavior observed for PET resin with DSC was found to be directly related to solid-state polymerization conditions. Multiple melting endothermic peaks were observed by others[6,23,24] and interpreted on the basis of distributions of crystal sizes or perfectness induced by thermal treatments.

References and Notes

(1) Bamford, C. H.; Wayne, P. R. *Polymer* **1969**, *10*, 661.
(2) Ravindranath, K.; Mashelkar R. A. *J. Appl. Polym. Sci.* **1990**, *39*, 1352.
(3) Schaaf, E.; Zimmerman, H.; Dietel, W.; Lohmann, P. *Acta Polym.* **1984**, *32*, 250.
(4) Chen, C. A.; Chen F. L. *J. Polym. Sci., Polym. Chem. Ed.* **1987**, *25*, 533.
(5) Jabarin, S. A.; Lofgen, E. A. *J. Appl. Polym. Sci.* **1986**, *32*, 5315.
(6) Chang, S.; Shen, M. F.; Chen, S. M. *J. Appl. Polym. Sci.* **1983**, *20*, 3283.
(7) Chang, T. M. *Polym. Eng. Sci.* **1970**, *10*, 364.
(8) Griskey, R. G.; Lee, B. I. *J. Appl. Polym. Sci.* **1966**, *10*, 105.
(9) Gaymans, R. J. *J. Polym. Sci., Polym. Chem. Ed.* **1985**, *23*, 1599.
(10) Yoon, K. H.; Kwon, M. H.; Jeon, M. H.; Park, O. O. *Polym. J.* **1993**, *25*, 219.
(11) Buxbaum, L. H. *J. Appl. Polym. Sci., Appl. Polym. Symp.* **1979**, *35*, 59.
(12) Pilati, F., In *Step Polymerization*; Eastmond, G. C., Ledwich, A., Russo, and Sigwalt, P., Eds.; Comprehensive Polymer Science, Vol. 5; Pergamon: New York, 1989; p 201.
(13) Ravindranath, K. *AIChE J.* **1984**, *30*, 415.
(14) Hovenkamp, S. G.; Munting, J. P. *J. Polym. Sci., Polym. Chem. Ed.* **1970**, *8*, 679.
(15) Hornof, V. *J. Macromol. Sci., Chem.* **1981**, *A15* (3), 503.
(16) Huang, G.; Wu, R.; Li, Y.; Zhang, D. *Hecheng Xianwei Gongye* **1991**, *4*, 31, (in Chinese).
(17) Buxbaum, L. H. *Angew. Chem., Int. Ed. Engl.* **1968**, *7*, 182.
(18) Ravindranath, K.; Mashelkar, R. A. *Chem. Eng. Sci.* **1986**, *41*. 2197.
(19) Chiu, W. Y.; Carratt, G. M.; Soong, D. S. *Macromolecules* **1983**, *16*, 384.
(20) Robert, W. H. *Numeral Methods*; Quantam Publishers Inc: New York, 1975.
(21) Van Krevelen, D. W. *Properties of Polymers*, 2nd ed.; Elsevier: Amsterdam, 1976.
(22) Branrup, J.; Immergut, E. H. *Polymer Handbook*, 3rd ed.; John Wiley: New York, 1989.
(23) Groennckx, F.; Ledent, J.; Berghmans, H. *J. Polym. Sci., Polym. Chem. Ed.* **1980**, *18*, 1311.
(24) Fontaine, F.; Ledent, J.; Groennckx, F. *Polymer* **1982**, *23*, 185.

MA9612541